

# Stimulus discrimination *via* responses of retinal ganglion cells and dopamine-dependent modulation

Hao Li, Pei-Ji Liang

School of Biomedical Engineering, Shanghai Jiao Tong University, Shanghai 200240, China

Corresponding author: Pei-Ji Liang. E-mail: [pjliang@sjtu.edu.cn](mailto:pjliang@sjtu.edu.cn)

© Shanghai Institutes for Biological Sciences, CAS and Springer-Verlag Berlin Heidelberg 2013

## ABSTRACT

Neighboring retinal ganglion cells (RGCs) fire with a high degree of correlation. It has been increasingly realized that visual perception of the environment relies on neuronal population activity to encode and transmit the information contained in stimuli. Understanding how neuronal population activity contributes to visual information processing is essential for understanding the mechanisms of visual coding. Here we simultaneously recorded spike discharges from groups of RGCs in bullfrog retina in response to visual patterns (checkerboard, horizontal grating, and full-field illumination) using a multi-electrode array system. To determine the role of synchronous activity mediated by gap junctions, we measured the correct classification rates of single cells' firing patterns as well as the synchronization patterns of multiple neurons. We found that, under normal conditions, RGC population activity exhibited distinct response features with exposure to different stimulus patterns and had a higher rate of correct stimulus discrimination than the activity of single cells. Dopamine (1  $\mu\text{mol/L}$ ) application did not significantly change the performance of single neuron activity, but enhanced the synchronization of the RGC population activity and decreased the rate of correct stimulus pattern discrimination. These findings suggest that the synchronous activity of RGCs plays an important role in the information coding of different types of visual patterns, and a dopamine-induced increase in synchronous activity weakens the population performance in pattern discrimination, indicating

the potential role of the dopaminergic pathway in modulating the population coding process.

**Keywords:** retinal ganglion cells; synchronous activity; dopamine; information coding

## INTRODUCTION

Perception of the environment relies on the ability of neurons to transmit signals effectively and encode/decode environmental stimuli efficiently. The population activity of neurons has been demonstrated to improve the transmission and coding processes<sup>[1-4]</sup>. In the retina, the correlated firing of ganglion cells plays an important role in visual signal transmission from the retina to the central visual areas<sup>[5]</sup> while correlated activity among large groups of cells is reflected by the correlated activity between pairs of neurons<sup>[6, 7]</sup>. Adjacent retinal ganglion cells (RGCs) frequently fire in a concerted manner, and these can be classified into different subtypes based on the spatiotemporal characteristics of the firing activity and the underlying mechanisms<sup>[3, 8]</sup>: (1) the correlated activity between RGCs induced by common inputs from pre-synaptic neurons, which has the property of distributed time lags in the cross-correlogram; and (2) the precisely synchronized firings in RGCs connected by gap junctions, which have a sharp peak a few milliseconds wide at zero-lag in the cross-correlogram. More than 50% of RGC spikes are involved in correlated and synchronized activity<sup>[3]</sup>, suggesting that the concerted activity may have a fundamental impact on the neuronal coding process.

It has been reported that the occurrence of synchronous

activity in direction-selective ON RGCs depends on the direction of stimulus motion, indicating that synchronization *via* gap junctions contributes to the encoding of stimulus information<sup>[9]</sup>. It is also known that gap junctional connectivity between RGCs is highly plastic, and can be effectively adjusted by the neuromodulator dopamine (DA)<sup>[10, 11]</sup>, resulting in changes of gap junctional conductance as well as the strength of synchronous activity<sup>[12, 13]</sup>. Yet, relatively little is known about whether synchronous activity among RGCs contributes to spatial visual pattern coding, and whether DA-induced changes in the gap-junction-coupled network affect the performance of the neuron population.

In the present study, we aimed to investigate the role of synchronous activity of RGCs in the information coding in response to different types of visual patterns and the effects of DA on this process. We used a multi-electrode array system to simultaneously record the spike sequences from a group of RGCs in bullfrog retina in response to visual stimuli with different spatial patterns (checkerboard, horizontal grating and full-field illumination). The rate of correct stimulation pattern discrimination was measured based on the RGC responses, both single neuron firing patterns and multi-neuronal synchronization patterns. Also, the neuronal activity during control and DA application were compared.

## MATERIALS AND METHODS

### Preparation

Bullfrogs were dark-adapted for 30 min prior to the experiments and freshly-isolated retinas were used for electrophysiological experiments. All procedures strictly conformed to the Humane Treatment and Use of Animals as prescribed by the Association for Research in Vision and Ophthalmology, and were approved by the Ethic Committee, School of Biomedical Engineering, Shanghai Jiao Tong University. Frogs were double-pithed under dim red light, and the eyes were enucleated. The eyeball was hemisected, the lens and cornea discarded, and the eye-cup cut into several pieces. The retina was carefully separated from the pigment epithelium<sup>[14]</sup> and immediately transferred onto a multi-electrode array (MEA60, MCS GmbH; Reutlingen, Germany) with the ganglion cell layer contacting the electrodes. The preparation was

superfused with normal oxygenated (95% O<sub>2</sub>, 5% CO<sub>2</sub>) Ringer containing (in mmol/L) 100.0 NaCl, 2.5 KCl, 1.6 MgCl<sub>2</sub>, 2.0 CaCl<sub>2</sub>, 25.0 NaHCO<sub>3</sub>, and 10.0 glucose. For pharmacological application, dopamine hydrochloride (1 μmol/L) (Sigma, St. Louis, MO) was added to the perfusate.

### Electrophysiological Recording

The multi-electrode array consisted of 60 electrodes (10 μm in diameter) in an 8 × 8 matrix (the 4 corners were left void) with horizontal and vertical adjacent tip-to-tip distances of 100 μm and a diagonal tip-to-tip distance of 141 μm. The tissue and perfusate were kept at room temperature (22–24°C). A small wired Ag/AgCl pellet was immersed in the bath solution and served as the reference electrode.

The firing activity of RGCs was simultaneously recorded by the multielectrode array system, and the signals were amplified through a 60-channel amplifier (single-ended, 1 200×, input impedance >10<sup>10</sup> Ω, output impedance 330 Ω). The neuronal signals from selected channels were sampled at 20 kHz (MC\_Rack, MCS GmbH) and stored in a computer. Spikes fired by individual cells were sorted using principal component analysis<sup>[15, 16]</sup>, and OfflineSorter software (Plexon Inc., Dallas, TX). To ensure accurate data for spatiotemporal pattern analysis, only single-neuron events identified by the above spike-sorting methods were used for further analyses<sup>[17, 18]</sup>.

### Stimulation

Visual stimuli were generated by a program written using the Matlab Psychophysics Toolbox<sup>[19]</sup> and displayed on a monitor (796 FD II, 1024×768 pixels, MAG Technology Co., Taipei). The visual image was focused on an area of 0.9 × 0.9 mm<sup>2</sup> when projected onto the isolated retina *via* a lens system.

Each trial consisted of three spatial patterns presented in random order: checkerboard (CB), horizontal grating (GT) and full-field illumination (FF) (Fig. 1). Each pattern was presented for 0.5 s at 1-s intervals. The CB consisted of 16 × 16 sub-squares (56 × 56 μm<sup>2</sup> in size), each randomly assigned “light” (12.18 nW/cm<sup>2</sup>) or “dark” (0.00 nW/cm<sup>2</sup>). The gratings contained eight “light” bars interleaved with eight “dark” bars (width × length of each bar: 56 × 896 μm<sup>2</sup>). A total of 100 trials were displayed at 1-s inter-trial-intervals. The same stimuli were applied in both the control and DA application tests.

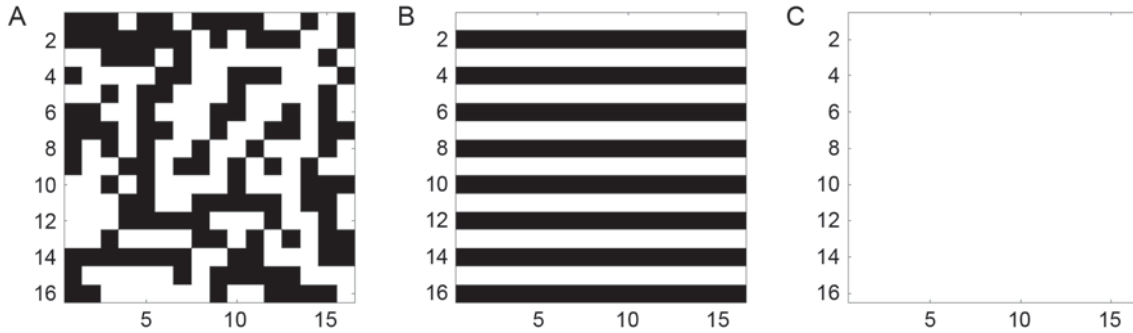


Fig. 1. Stimulus patterns. A: Checkerboard. B: Horizontal grating. C: Full-field illumination.

### Synchronous Neuron Groups and Synchronization Strength

For a target neuron  $a$  under investigation, shift-predicted cross-correlograms paired with its neighboring neurons were computed as:

$$\hat{C}_{ak}(t) = \frac{C_{ak}(t) - C_{ak}^{shifted}(t)}{\sqrt{f_a f_k}} (t \in [-L, L] \quad k = 1, 2, \dots, N)$$

where  $C_{ak}(t)$  and  $C_{ak}^{shifted}(t)$  are the raw and shifted cross-correlograms between neurons  $a$  and  $k$ <sup>[20, 21]</sup>;  $\hat{C}_{ak}(t)$  denotes the shift-predicted cross-correlogram with jitter of 1 ms;  $t$  and  $L$  represent the time-lag and its maximal value in the cross-correlogram computation;  $f_a$  and  $f_k$  are the firing rates of neurons  $a$  and  $k$ , respectively;  $N$  is the number of neighboring neurons whose activity is synchronized with neuron  $a$ . In our calculation, the synchronization strength of neuron pairs was normalized against the firing rates, which minimized the dependence of synchronization estimation on firing rate.

Based on the cross-correlogram estimations, synchronized pairs were identified as those with a central peak width  $< 2$  ms and a peak value  $> 0.1$  arbitrary unit (Fig. 2B)<sup>[13]</sup>. A target RGC with all its synchronized neighbors was defined as a “synchronous neuron group”. The synchronization strength of the group was defined as the averaged pair-wise synchronization strength between the target neuron  $a$  and its neighbors:

$$\bar{C}_a = \frac{1}{K} \sum_{j=1}^K \max[\hat{C}_{aj}(t)] (t \in [-L, L])$$

where  $K$  is the number of identified neurons with activity synchronized with neuron  $a$ .

### Integrated Multi-neuronal Spiking Sequence

To estimate the contribution of population activity to stimulus discrimination, we defined an integrated multi-neuronal spiking sequence as follows: in a synchronized group (consisting of  $K$  neurons), spike trains of all the group members were binned into 2-ms time windows, and represented in a binary manner:

$$r_t^j = \begin{cases} 1, & \text{if neuron } j \text{ fired a spike in bit } t \\ 0, & \text{otherwise} \end{cases}$$

$j = 1, \dots, K$ ;  $t = 1, \dots, m$  (where  $m$  is the length of the sequence).

The integrated sequence  $S(t)$  was reconstructed as:

$$S(t) = \frac{\sum_{j=1}^K r_t^j}{K}.$$

Fig. 3 shows the construction of an integrated sequence. The values in the sequence ranged from 0 to 1, denoting the degree of synchronization in the neuron group.

### Classification of Neuronal Response Patterns Based on the Support Vector Machine (SVM) Method

To assess the performance of RGCs in stimulus pattern discrimination, we performed classification analysis based on single and population neuronal activity. Each trial of a single neuron spike train ( $r_t^j$ ) or the integrated sequence ( $S(t)$ ) of a synchronous group (Fig. 3B) was presented as a point in  $m$ -dimensional space (where  $m$  is the length of the sequence). The classification was to cluster these data points and assign each point to a corresponding pattern in response to a particular stimulus.

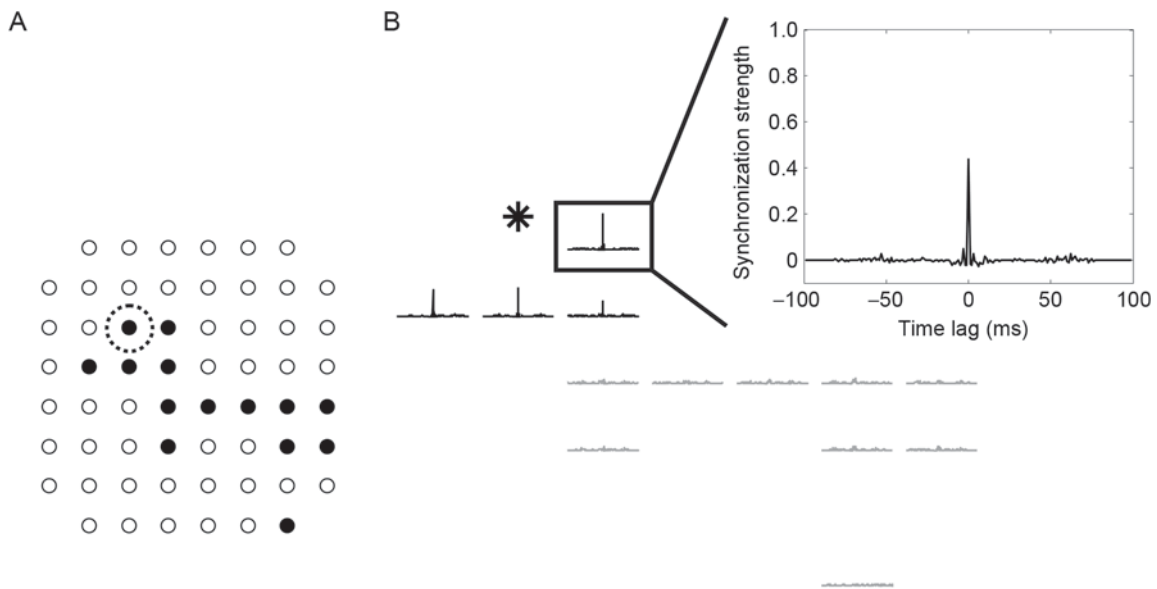


**Fig. 2. A:** Locations of electrodes by which 14 retinal ganglion cells (RGCs) were recorded (filled circles). Target cell indicated by the dashed circle. **B:** Shift-predicted cross-correlogram of the target cell (asterisk) paired with those of the other 13 cells. Synchronization was found between the target cell and four of its neighbors (black traces), so this synchronous group consisted of five RGCs. Gray plots show the neuron pairs with no significantly synchronized activity. Inset: time lag and strength of the shift-predicted cross-correlogram.

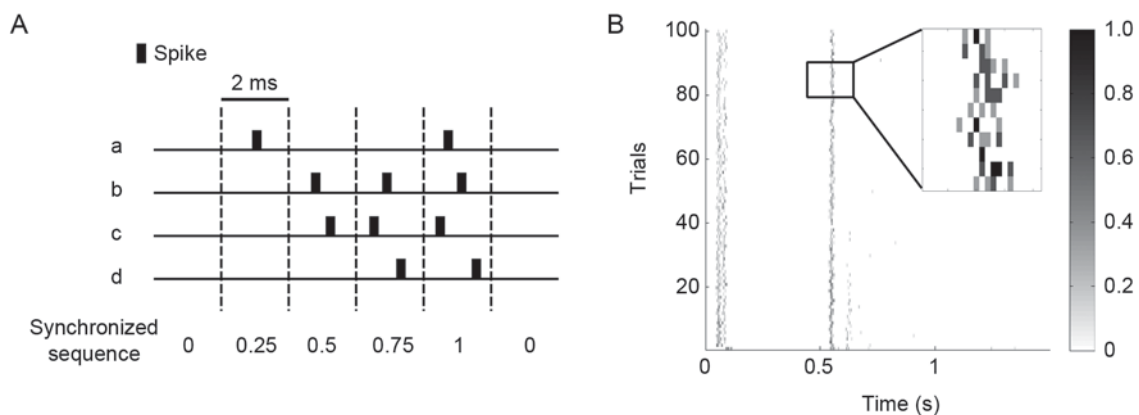


**Fig. 3. Construction of an integrated multi-neuronal spiking sequence. A:** Spike trains of neurons a, b, c and d, and the integrated sequence derived from this data set. **B:** An example of the integrated sequence from a 4-neuron group. Inset: Enlarged details, with the sequence values represented by the gray scale.

We used the SVM method (Matlab built-in toolbox) to identify the neuronal activity in response to different stimuli as represented by data clusters in  $m$ -dimensional space. SVMs construct a hyper-plane (known as the maximal margin hyper-plane) that is the optimal separation of binary-labeled training data<sup>[22–24]</sup>. The procedure of classifying the neuronal responses to two distinct patterns

a and b ( $P_a$  and  $P_b$ ) consisted of two steps: (1) The hold-out cross-validation experiment. Since adaptation occurred when the retina was exposed to repeated patterns, we selected the data collected during steady-state responses for further analysis to minimize the adaptation effects. The results of the first 10 trials were discarded, and the remaining 90 trials were used. To build up the training data,

half of the 90 neuronal responses in our experimental data were randomly selected from the responses to  $P_a$  and  $P_b$ , and the remaining 45 responses were used as test data. (2) Training the SVM classifier with the training data to work out the maximal margin hyper-plane that separates the neuronal responses to  $P_a$  and  $P_b$  into two classes. Then the test data were classified by the trained classifier (the hyper-plane), and the ratio of the correctly-labeled trials (the number correct/90) was calculated. In our analysis, for a single spike train ( $r_i^j$ ) (or an integrated sequence  $S(t)$ ) in response to patterns  $a$  and  $b$ , the classification procedures (1) and (2) described above were independently repeated 10 times, and the average value of the correct ratio was determined as the rate of correct classification based on ( $r_i^j$ ) (or  $S(t)$ ) between  $P_a$  and  $P_b$ .

For each paired pattern (CB vs GT, CB vs FF, and GT vs FF), the classification procedure was performed based on the single neuron spike train ( $r_i^j$ ) and the integrated sequence ( $S(t)$ ).

## RESULTS

### Single Neuron Activity and Integrated Sequence

Typical responses of an RGC elicited by the three patterns

(CB, GT and FF) are plotted in Fig. 4A. Both with and without DA application (1  $\mu\text{mol/L}$ ), this RGC exhibited transient responses when the stimulus pattern was switched ON and OFF. Only those cells exhibiting the same ON-OFF transient responses and good stability (as in Fig. 4A) were chosen for further investigation. The mean firing rate (spikes per second) averaged from 58 single neurons in five retinas showed clear differences across the CB, GT and FF patterns (Fig. 4B), with the highest firing rate to CB, intermediate to GT and lowest to FF.

An example of the integrated sequence of a 4-neuron synchronous group, in which the degree of synchronized activity is represented by the gray scale, is shown in Fig. 5.

For each retina under investigation, the number of RGCs that could be recorded ranged from 5 to 20 (7, 5, 20, 12, and 14 for retinas 1–5, respectively), and the group size for the synchronized neurons also varied (Fig. 6).

### Classification of Stimulus-pattern-dependent Neuronal Activity

As RGCs transform different stimulus patterns into spikes, the stimulus features should be characterized by the neuronal response properties. Here, we used the SVM method to classify the neuronal response patterns.

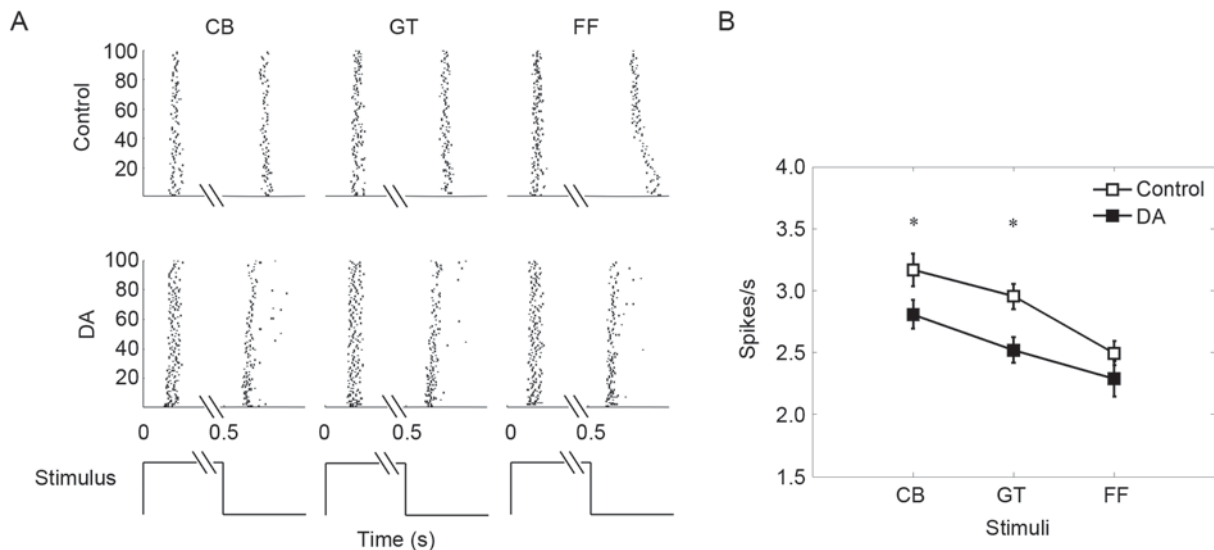
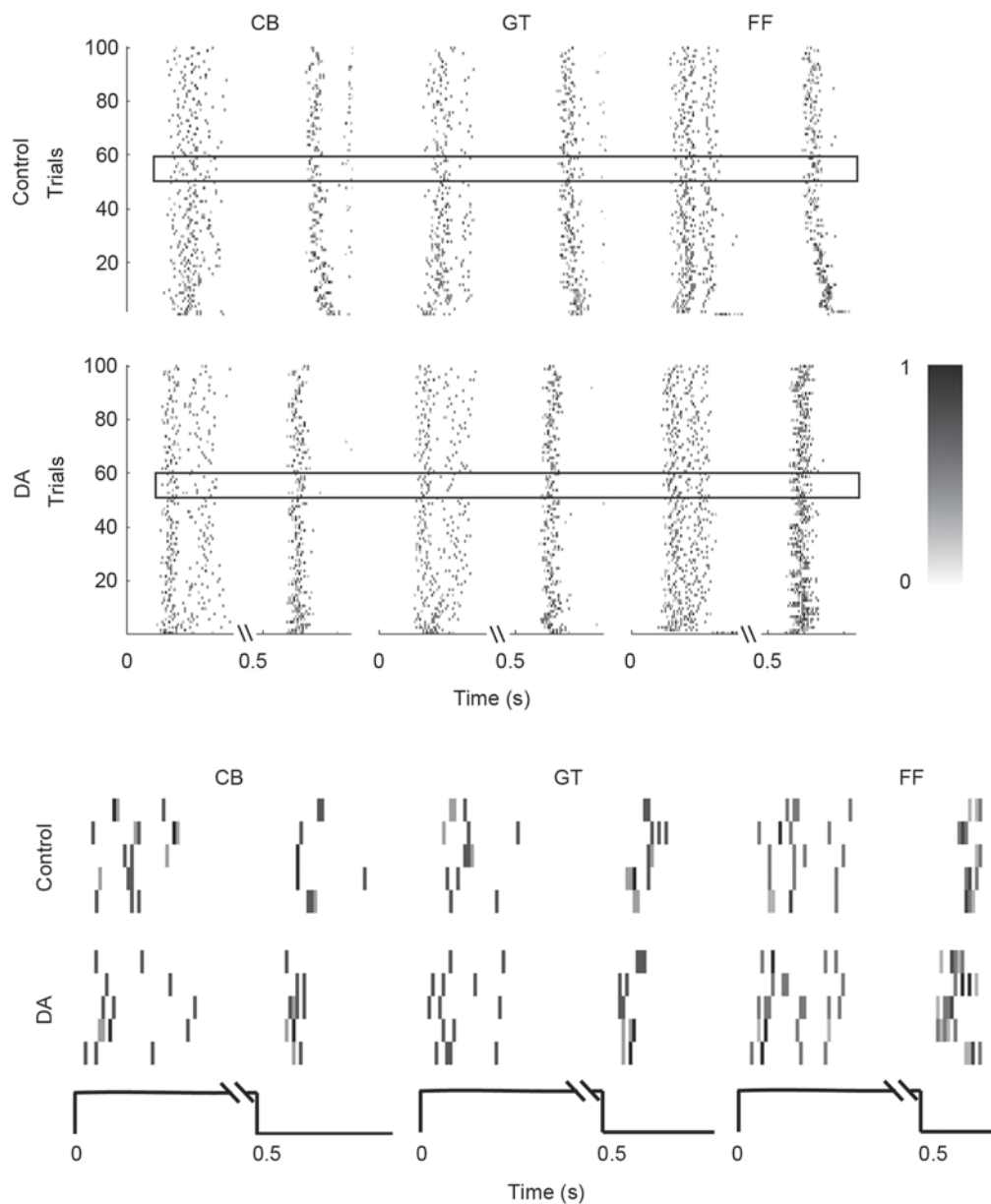


Fig. 4. Single neuron firing activity. A: Responses of an RGC to checkerboard (CB), horizontal grating (GT) and full-field illumination (FF) in controls and during 1  $\mu\text{mol/L}$  dopamine (DA) application, with the stimulus presented at 0.5 s-ON/1 s-OFF and repeated 100 times (bottom: stimulus time-course). Each dot represents a spike. B: Firing rate averaged across 58 neurons from five retinas in response to CB, GT and FF in controls and during DA application. Data are mean  $\pm$  SE. \* $P < 0.05$  vs DA, paired  $t$ -test.



**Fig. 5.** An example of integrated multi-neuronal spiking sequences for a 4-neuron group. Top panels: 100 trials of integrated sequences in response to checkerboard (CB), horizontal grating (GT) and full-field illumination (FF) in controls and during DA ( $1 \mu\text{mol/L}$ ) application. Bottom panels: Enlarged details of the trials in the rectangles in the top panels. The sequence values are represented by the gray scale. Bottom traces show the stimulus time-course.

The computation based on single neuron spike trains ( $r_i^j$ ) showed that, in controls, the mean correct rates were  $0.566 \pm 0.006$  for discriminating CB vs GT,  $0.742 \pm 0.009$  for CB vs FF and  $0.743 \pm 0.008$  for GT vs FF (mean  $\pm$  SE) (Fig. 7A, C–E) (58 neurons from five retinas).

To estimate the population neuron performance,

integrated sequences  $S(t)$  (as shown in Fig. 5) were used to compute the correct rate. The mean values for correct rate in controls were  $0.598 \pm 0.010$  for CB vs GT,  $0.828 \pm 0.008$  for CB vs FF and  $0.829 \pm 0.010$  for GT vs FF (44 groups from five retinas) (Fig. 7B). All were higher than the single neuron correct rate ( $P < 0.05$ , unpaired  $t$ -test;

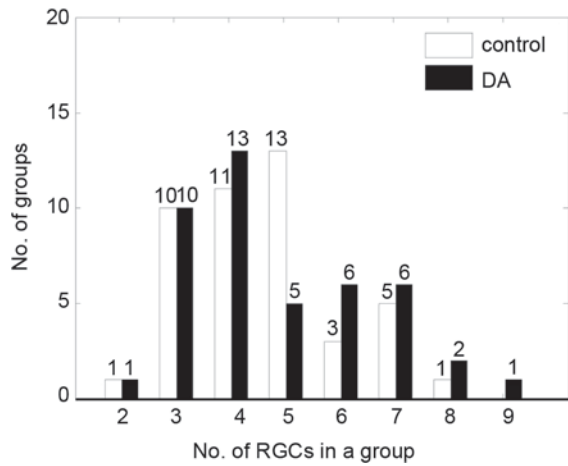


Fig. 6. Histogram of the size of synchronized neuron groups in controls and during DA application.

Fig. 7C–E), showing that the population activity performed better in pattern discrimination.

It has been demonstrated that the coding performance of a synchronous group is related to the number of neurons in the group<sup>[5]</sup>. To probe the potential relationship between discrimination performance and the number of RGCs in the group, we plotted the correct rate against the number of RGCs in each synchronous group (Fig. 8A-C). The linear relationship between the correct rate against RGC group size showed that in control conditions, the performance of synchronous groups was positively correlated with group size.

**DA-induced Effects on Correct Rates of Single Neurons and Synchronous Groups**

DA is a neuronal modulator released in the retina by light.

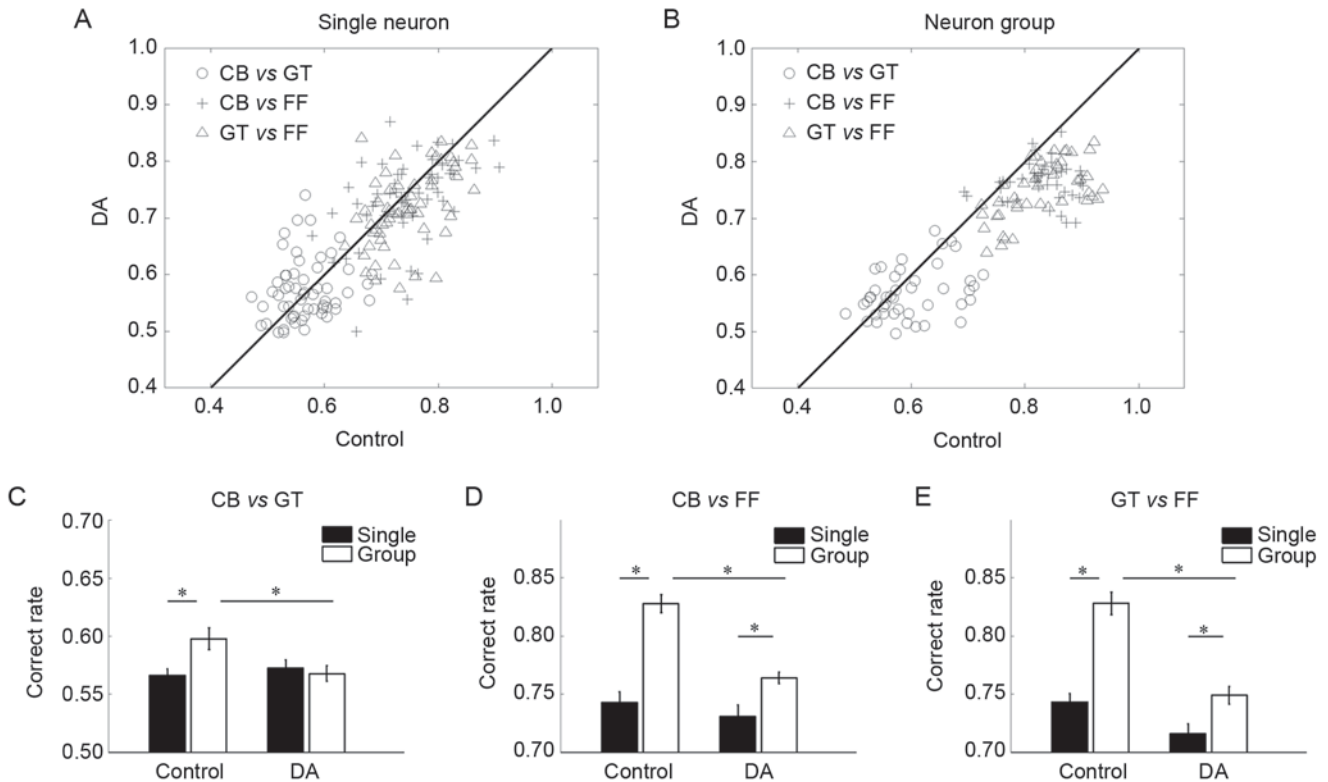
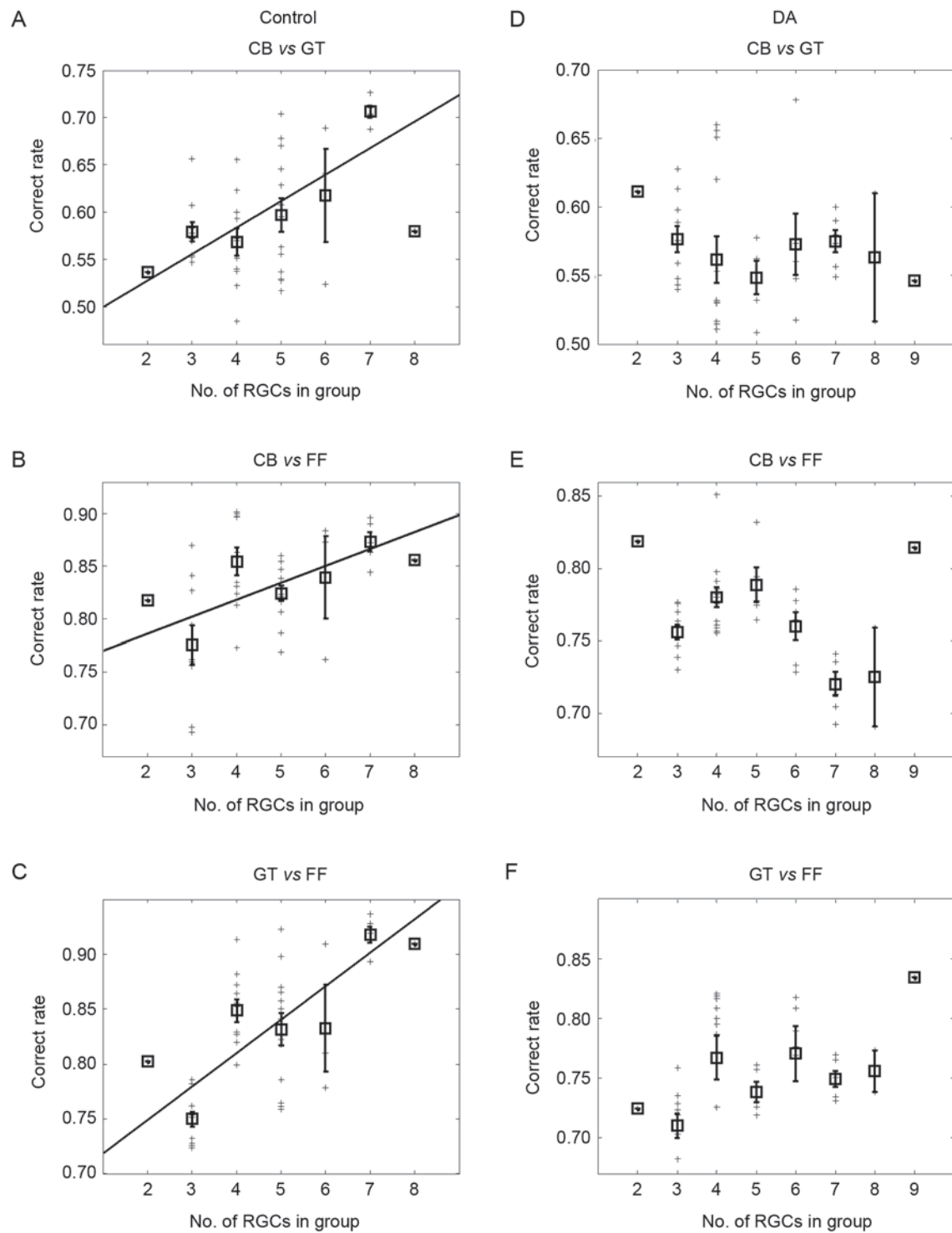


Fig. 7. Correct rates of single neurons and neuron groups in pattern discrimination. A: Correct rate of single neuron activity (58 neurons from five retinas) in discriminating the patterns checkerboard (CB) vs horizontal gratings (GT), CB vs full-field illumination (FF), and GT vs FF. Each point denotes the correct rate of an RGC. B: Correct rate of population neuron activity (44 groups from five retinas) in discriminating the patterns CB vs GT, CB vs FF, and GT vs FF. Each point denotes the correct rate of an RGC group. C–E: Correct rates in single neurons and neuron groups for pattern discrimination of CB vs GT (C), CB vs FF (D), and GT vs FF (E) with/without DA application. Mean  $\pm$  SE. \* $P < 0.05$  based on paired and unpaired  $t$ -tests .



**Fig. 8.** Plots of correct rate vs synchronous RGC group size. A–C: The correct rates of 44 groups with varied numbers of RGCs in control conditions. The fitted lines demonstrate a linear correlation between rate and size. (A) CB vs GT,  $R = 0.572$ ,  $P < 0.05$ ; (B) CB vs FF,  $R = 0.436$ ,  $P < 0.05$ ; (C) GT vs FF,  $R = 0.673$ ,  $P < 0.05$ . D–F: The correct rates of 44 groups with varied numbers of RGCs during DA application. (D) CB vs GT,  $R = -0.006$ ,  $P > 0.05$ ; (E) CB vs FF,  $R = -0.300$ ,  $P > 0.05$ ; (F) GT vs FF,  $R = 0.231$ ,  $P > 0.05$ . '+' indicates the correct rate of the corresponding group. The squares and error bars are mean and SE respectively.

It participates in the regulation of intracellular chemical pathways in single neurons<sup>[25]</sup> and of inter-neuronal gap junctions<sup>[11]</sup>. In particular, the gap-junction-dependent synchronous activity of RGCs is modulated by DA<sup>[11, 13]</sup>, suggesting that it is involved in the population coding process. Here, we investigated whether exogenous DA (1  $\mu\text{mol/L}$ ) affects the performance of single neurons and synchronous neuronal groups in stimulus pattern discrimination.

The spike sequences of a representative RGC with/without DA application are shown in Fig. 4. Clearly, in the presence of DA, the neuron exhibited typical transient responses to the ON and OFF stimulus pattern, similar to controls. A comparison of the two conditions showed that the mean firing rate in response to each stimulus pattern was reduced during DA application ( $P < 0.05$  for CB and GT, paired  $t$ -test, Fig. 4B). During DA application, the mean correct rates of single neurons were  $0.572 \pm 0.007$  for CB vs GT,  $0.731 \pm 0.010$  for CB vs FF, and  $0.716 \pm 0.009$  for GT vs FF (58 neurons from five retinas), with no significant difference from the control (Fig. 7A, C–E). These results suggested that, although DA decreased the firing rates of single neurons in response to each pattern, the temporal structure of the firing sequences were similar to the control.

The correct rates of pattern discrimination of RGC groups during DA application were computed based on integrated sequences  $S(t)$  as shown in Fig. 5. Among 44 synchronous groups from five retinas during DA application,

the mean correct rates were  $0.568 \pm 0.007$  for CB vs GT,  $0.764 \pm 0.005$  for CB vs FF, and  $0.749 \pm 0.008$  for GT vs FF (Fig. 7B, C–E), which were all lower than the correct rates in control conditions ( $P < 0.05$ , paired  $t$ -test). This suggested that DA down-regulates the discriminatory performance of synchronous groups.

In addition, DA application eliminated the linear association between the correct rate and the size of synchronous RGCs groups observed during control conditions (Fig. 8D–F).

### Synchronization Strength Increased by DA

Since the integrated sequence  $S(t)$  was constructed based on the synchronized activity *via* gap junctions among the coupled RGCs, which is modulated by DA<sup>[3, 26]</sup>, it is thus reasonable to speculate that down-regulation of neuron group performance in pattern discrimination is probably related to the DA-induced effects on synchronous activity. We therefore further examined the strength of synchronization.

RGCs with significant synchronous firing were defined as a synchronous group, and the synchronization strength ( $\bar{C}_a$ ) of the group was estimated with/without DA. The mean values for  $\bar{C}_a$  across the 44 groups during control were  $0.460 \pm 0.016$  (CB),  $0.470 \pm 0.018$  (GT),  $0.431 \pm 0.019$  (FF). During DA application, the mean values for  $\bar{C}_a$  were  $0.565 \pm 0.023$  (CB),  $0.580 \pm 0.023$  (GT),  $0.570 \pm 0.023$  (FF) (Fig. 9). The synchronization strength was increased during DA

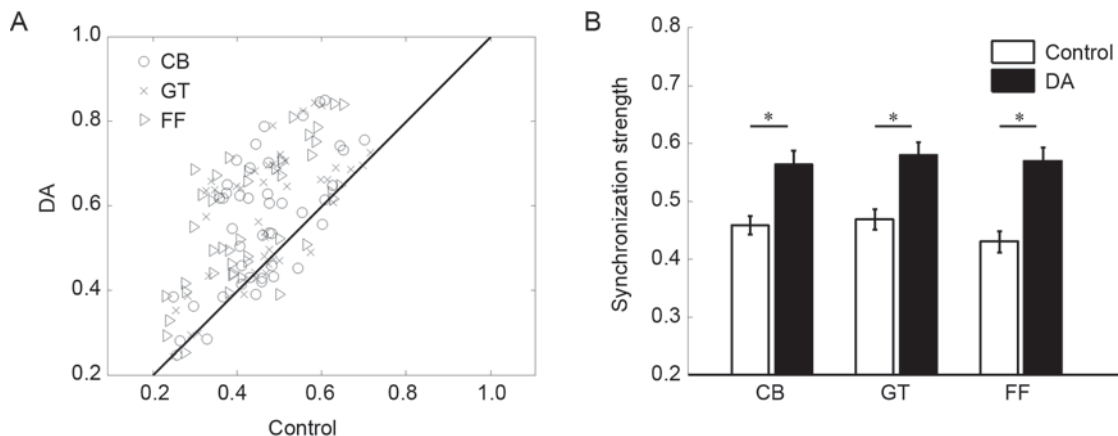


Fig. 9. Synchronization strength of neuron groups. A: Synchronization strength of 44 groups from five retinas with/without DA application in response to checkerboard (CB), horizontal grating (GT) and full-field illumination (FF). B: Statistical summary. Mean  $\pm$  SE. \* $P < 0.05$ , paired  $t$ -test.

application for all the three patterns (all  $P < 0.05$ , paired  $t$ -test). These results are consistent with our previous study that DA enhances RGC-RGC gap junctional connections, resulting in increased synchronization<sup>[13]</sup>.

## DISCUSSION

We investigated the activity of single neurons and neuron groups in response to different visual patterns and found that under control conditions, neuron groups performed better in visual pattern coding than single neurons. In addition, the correct rate of neuron groups was positively correlated with group size. However, the performance of neuron groups was significantly reduced by DA application, while that of single neurons was not altered. Furthermore, DA eliminated the positive correlation between neuron group performance and group size in all three cases (CB vs GT, CB vs FF, and GT vs FF). The DA-induced enhancement of synchronization may be the mechanism underlying the performance changes in the neuron groups. In addition, the decay time-constant indicated that the firing rate of the majority of neurons declined to a steady state within 10 trials. We also assessed the neuronal performance using all 100 trials, and the results were consistent with the findings based on our selection criteria (data not shown).

### Visual Pattern Coding with Single and Population Activity

RGCs encode stimulus patterns with firing responses, and exhibit specific firing patterns to stimulus features such as light intensity, contrast, and texture. The stimulus-response relationship based on firing patterns facilitates the identification of visual inputs and the decoding of information by downstream neurons. Thus, the firing patterns, both of single neurons and populations, are crucial for the visual perception process.

In the present study, the activity of both single neurons and populations showed stimulus-related features in response to different visual patterns, showing the contribution of specific patterns in single neuronal spiking sequences and the integrated multi-neuronal spiking sequences to visual information coding. For single neurons, the temporal structure of the sequence probably contributes to the encoding of specific patterns<sup>[27]</sup>.

Under control conditions, the neuron groups exhibited a higher rate of correct pattern discrimination than single neurons. One explanation could be that the integrated sequence  $S(t)$  averaged out inter-neuronal response noise. But at the same time, the temporal structure of the firing of multiple neurons was dynamically modulated by the different stimulus patterns and these changes were reflected by the integrated sequence. When exposed to visual stimuli, the synchronization strength is unequally distributed across the neuronal subsets, and depends on the stimulus pattern that covers the mosaic of multi-neuronal receptive fields<sup>[28]</sup>. The elements of the integrated sequence varied with finer details for representing response features, and therefore performed better in stimulus discrimination. The synchronization of neuron groups provides an extended information coding capacity to describe the difference between the stimulus patterns and enhances neurons' capacity for specific pattern identification, which is consistent with the notion that correlation among neuron population activity improves coding efficiency and information transmission<sup>[1, 2, 5, 29]</sup>.

Correspondingly, the correct rate of neuron groups was linearly correlated with the number of neurons in the group. In fact, the number of neurons in a synchronous group reflects the dimension of the multi-neuronal data, and if these data span more independent dimensions, the features in the data are projected onto an extended space, which increases the probability for these features to be clearly separated and the corresponding patterns to be correctly encoded.

### Dopamine-induced Effects on Synchronous Activity

To determine the role of synchronization in visual pattern coding, we applied exogenous DA to the retina to manipulate the synchronization state of neuron groups<sup>[12, 13]</sup>.

The neuromodulator DA, which is released by amacrine and interplexiform cells under photopic conditions<sup>[30]</sup>, activates intracellular signal pathways involving cAMP-dependent protein kinase, which modifies the gap junction connexins and changes their permeability to ionic currents<sup>[11]</sup>. In single neurons, the performance did not significantly change during DA application. But in the neuron groups, DA application decreased the rate of correct pattern discrimination, and eliminated the linear correlation between correct rate and group size.

The persistence of performance in single neurons during DA application might be due to minor changes in the temporal structure of the firing sequences. In the neuron groups, the synchronization strength was significantly increased by DA in all three patterns (Fig. 9), consistent with our previous finding that DA enhances RGC-RGC gap junctional connections *via* the activation of D1 receptors and results in increased synchronization<sup>[13]</sup>. Application of 1  $\mu\text{mol/L}$  DA induces a much higher concentration in the retina than under natural conditions<sup>[31]</sup>, such that it remains at a constant high level. So the dynamic modulation of DA concentration in the retina was eliminated. Therefore, the DA-related dynamics of synchronized activity under control conditions was disrupted by DA application and the performance of neuron groups in visual pattern coding was weakened. Our results suggest that, although synchronization promotes the coding efficiency of neuron populations in some sensory processes, the exogenous DA-induced loss of dynamic modulation of synchronized activity results in the attenuation of stimulus-response specificity in pattern discrimination, thereby weakening the neuronal ability to encode different stimulus patterns. Thus, the dynamic modulation of synchronization is essential for neuron populations to optimize the coding process.

In summary, our results suggest that population activity enhances the visual pattern coding of neurons. DA may be an important neuromodulator involved in the modulation of RGC population activity, and plays a critical role in maintaining the responsiveness and information coding of neurons.

## ACKNOWLEDGMENTS

We thank Xin-Wei Gong and Hai-Qing Gong for important technical contributions. This work was supported by a grant from the National Natural Science Foundation of China (61075108).

Received date: 2012-09-21; Accepted date: 2013-01-26

## REFERENCES

- [1] Pillow JW, Shlens J, Paninski L, Sher A, Litke AM, Chichilnisky EJ, *et al.* Spatio-temporal correlations and visual signalling in a complete neuronal population. *Nature* 2008, 454: 995–999.
- [2] Koch K, McLean J, Berry M, Sterling P, Balasubramanian V, Freed MA. Efficiency of information transmission by retinal ganglion cells. *Curr Biol* 2004, 14: 1523–1530.
- [3] Brivanlou IH, Warland DK, Meister M. Mechanisms of concerted firing among retinal ganglion cells. *Neuron* 1998, 20: 527–539.
- [4] Mastrorarde DN. Correlated firing of retinal ganglion cells. *Trends Neurosci* 1989, 12: 75–80.
- [5] Schnitzer MJ, Meister M. Multineuronal firing patterns in the signal from eye to brain. *Neuron* 2003, 37: 499–511.
- [6] Schneidman E, Berry MJ 2nd, Segev R, Bialek W. Weak pairwise correlations imply strongly correlated network states in a neural population. *Nature* 2006, 440: 1007–1012.
- [7] Nirenberg S, Latham PE. Decoding neuronal spike trains: how important are correlations? *Proc Natl Acad Sci U S A* 2003, 100: 7348–7353.
- [8] Meister M, Lagnado L, Baylor DA. Concerted signaling by retinal ganglion cells. *Science* 1995, 270: 1207–1210.
- [9] Ackert JM, Wu SH, Lee JC, Abrams J, Hu EH, Perlman I, *et al.* Light-induced changes in spike synchronization between coupled ON direction selective ganglion cells in the mammalian retina. *J Neurosci* 2006, 26: 4206–4215.
- [10] Mills SL, Xia XB, Hoshi H, Firth SI, Rice ME, Frishman LJ, *et al.* Dopaminergic modulation of tracer coupling in a ganglion-amacrine cell network. *Vis Neurosci* 2007, 24: 593–608.
- [11] Bloomfield SA, Volgyi B. The diverse functional roles and regulation of neuronal gap junctions in the retina. *Nat Rev Neurosci* 2009, 10: 495–506.
- [12] Hu EH, Pan F, Volgyi B, Bloomfield SA. Light increases the gap junctional coupling of retinal ganglion cells. *J Physiol* 2010, 588: 4145–4163.
- [13] Li H, Liu WZ, Liang PJ. Adaptation-dependent synchronous activity contributes to receptive field size change of bullfrog retinal ganglion cell. *PLoS One* 2012, 7: e34336.
- [14] Jing W, Liu WZ, Gong XW, Gong HQ, Liang PJ. Visual pattern recognition based on spatio-temporal patterns of retinal ganglion cells' activities. *Cogn Neurodyn* 2010, 4: 179–188.
- [15] Wang GL, Zhou Y, Chen AH, Zhang PM, Liang PJ. A robust method for spike sorting with automatic overlap decomposition. *IEEE Trans Biomed Eng* 2006, 53: 1195–1198.
- [16] Zhang PM, Wu JY, Zhou Y, Liang PJ, Yuan JQ. Spike sorting based on automatic template reconstruction with a partial solution to the overlapping problem. *J Neurosci Methods* 2004, 135: 55–65.
- [17] Chen AH, Zhou Y, Gong HQ, Liang PJ. Firing rates and dynamic correlated activities of ganglion cells both contribute to retinal information processing. *Brain Res* 2004, 1017: 13–20.
- [18] Liu X, Zhou Y, Gong HQ, Liang PJ. Contribution of the GABAergic pathway(s) to the correlated activities of chicken

- retinal ganglion cells. *Brain Res* 2007, 1177: 37–46.
- [19] Brainard DH. The Psychophysics Toolbox. *Spat Vis* 1997, 10: 433–436.
- [20] Perkel DH, Gerstein GL, Moore GP. Neuronal spike trains and stochastic point processes. II. Simultaneous spike trains. *Biophys J* 1967, 7: 419–440.
- [21] Pauluis Q, Baker SN, Olivier E. Precise burst synchrony in the superior colliculus of the awake cat during moving stimulus presentation. *J Neurosci* 2001, 21: 615–627.
- [22] Brown MP, Grundy WN, Lin D, Cristianini N, Sugnet CW, Furey TS, *et al.* Knowledge-based analysis of microarray gene expression data by using support vector machines. *Proc Natl Acad Sci U S A* 2000, 97: 262–267.
- [23] Furey TS, Cristianini N, Duffy N, Bednarski DW, Schummer M, Haussler D. Support vector machine classification and validation of cancer tissue samples using microarray expression data. *Bioinformatics* 2000, 16: 906–914.
- [24] Noble WS. What is a support vector machine? *Nat Biotechnol* 2006, 24: 1565–1567.
- [25] Witkovsky P. Dopamine and retinal function. *Doc Ophthalmol* 2004, 108: 17–40.
- [26] Hu EH, Bloomfield SA. Gap junctional coupling underlies the short-latency spike synchrony of retinal alpha ganglion cells. *J Neurosci* 2003, 23: 6768–6777.
- [27] Liu WZ, Jing W, Li H, Gong HQ, Liang PJ. Spatial and temporal correlations of spike trains in frog retinal ganglion cells. *J Comput Neurosci* 2011, 30: 543–553.
- [28] Neuenschwander S, Singer W. Long-range synchronization of oscillatory light responses in the cat retina and lateral geniculate nucleus. *Nature* 1996, 379: 728–732.
- [29] Liu WZ, Yan RJ, Jing W, Gong HQ, Liang PJ. Spikes with short inter-spike intervals in frog retinal ganglion cells are more correlated with their adjacent neurons' activities. *Protein Cell* 2011, 2: 764–771.
- [30] Witkovsky P, Deary A. Functional roles of dopamine in the vertebrate retina. *Prog Retinal Res* 1991, 11: 247–292.
- [31] Witkovsky P, Nicholson C, Rice ME, Bohmaker K, Meller E. Extracellular dopamine concentration in the retina of the clawed frog, *Xenopus laevis*. *Proc Natl Acad Sci U S A* 1993, 90: 5667–5671.